Some Effects of Stratification on Long Trench Waves[1]

K. H. BRINK

Woods Hole Oceanographic Institution, Woods Hole, MA 02543

(Manuscript received 30 August 1982, in final form 29 November 1982)

ABSTRACT

The characteristics of long, gravest mode trench waves in the presence of realistic stratification are investigated. Two examples are computed, representing cases with widely differing importance of baroclinic effects. In both cases, the wave-related alongshore velocity structure becomes noticeably bottom intensified, but much less so for the high latitude (smaller internal Rossby radius of deformation) Aleutian trench example than for the low latitude (larger Rossby radius) Peru trench example. Some consequences of the bottom trapping are then discussed.

1. Introduction

Recent papers by Mysak *et al.* (1979) and by Mysak and Willmott (1981) (hereafter referred to as MLE and MW, respectively) have treated barotropic trench waves. These low frequency vorticity waves have the same essential physics as barotropic continental shelf waves (e.g., Gill and Schumann, 1974) but are largely confined to submarine trenches at the base of the continental slope. It is useful to consider the effects of realistic continuous stratification on these waves since, for example, Huthnance (1978) and Chapman and Henderschott (1982) have shown that wave properties can change drastically when baroclinicity is included. In the following, the properties of free and forced long trench waves with stratification will be considered, and two baroclinic examples, treated by MLE and MW under the barotropic assumption, will be discussed.

2. Method

We consider a stably stratified fluid in a semi-infinite basin rotating about its vertical axis at an angular frequency $f/2$. The right-handed coordinate system is chosen as x offshore, y alongshore and z upwards. The coast is at $x = 0$, and the surface at $z = 0$. Completely linear, Boussinesq dynamics are assumed. The depth of the fluid is $h(x)$, and the Brunt–Väisälä frequency is $N(z)$. The depth is assumed to increase monotonically from the coast to the trench bottom, and then to decrease monotonically until the ocean bottom becomes flat. An alongshore wind stress $\tau_0^y(y, t)$ is applied at the surface. Finally, the long wave assumption is made, i.e., that time scales are long relative to f^{-1}, and that alongshore spatial scales are long relative to those in the x direction.

Under these assumptions, the governing equations are

$$-fv = -\rho_0^{-1}p_x, \tag{2.1a}$$

$$v_t + fu = -\rho_0^{-1}p_y + Y_s, \tag{2.1b}$$

$$0 = -p_z - g\rho, \tag{2.1c}$$

$$0 = u_x + v_y + w_z, \tag{2.1d}$$

$$0 = \rho_t + w\bar{\rho}_z, \tag{2.1e}$$

where p is pressure, g the acceleration due to gravity, and u, v, and w are the velocity components in the x, y and z directions, respectively. Subscripts x, y, z, t denote partial differentiation. The density is taken as

$$\rho = \rho_0 + \bar{\rho}(z) + \rho(x, y, z, t). \tag{2.2}$$

Finally, following Clarke (1977), the surface layer stress gradient is given as

$$Y_s = (\rho_0 h_M)^{-1} H(h_M + z)\tau_0^y(y, t), \tag{2.3}$$

where h_M is the surface layer depth (taken to be such that $h_M < h(x)$ for all x) and $H(\xi)$ is the Heaviside unit function.

Given the formulation, it is straightforward to express the problem in terms of the single dependent variable p. The general solution can then be expressed as

$$p = \sum_{n=-\infty}^{\infty} F_n(x, z)\phi_n(y, t), \tag{2.4}$$

where the bounds on the sum reflect the fact that the free waves can propagate in both the positive and

[1] WHOI Contribution No. 5207.

negative directions. The free long wave modal structures F_n are defined by the eigenvalue problem:

$$F_{nxx} + f^2\left(\frac{F_{nz}}{N^2}\right)_z = 0, \tag{2.5a}$$

$$F_{nz} = 0, \quad \text{at} \quad z = 0, \tag{2.5b}$$

$$F_{nz} + N^2 h_x f^{-2}(F_{nx} + f c_n^{-1} F_n) = 0, \quad \text{at} \quad z = -h(x), \tag{2.5c}$$

$$F_{nx} + f c_n^{-1} F_n = 0, \quad \text{at} \quad x = 0, \tag{2.5d}$$

$$F_n \to 0, \quad \text{as} \quad x \to \infty. \tag{2.5e}$$

The first condition [(2.5b)] represents a rigid lid at the upper boundary; the second and third [(2.5c), (2.5d)], no normal flow at solid boundaries; and the fourth [(2.5e)], coastal trapping. The long-wave phase velocity c_n is the eigenvalue. The eigenfunctions are orthogonal according to

$$\delta_{nm} = \int_{-h}^{0} F_n F_m dz\Big|_{x=0} + \int_0^{\infty} h_x F_n F_m dx\Big|_{z=-h}, \tag{2.6}$$

where δ_{nm} is the Kronecker delta. Note that (2.6) requires that the F_n have the somewhat unusual units of (length)$^{-1/2}$. Finally, the wave amplitudes are governed by

$$\phi_{ny} - c_n^{-1}\phi_{nt} = b_n \tau_0^y, \tag{2.7a}$$

where

$$b_n = (h_M)^{-1} \int_{-h_M}^{0} F_n dz\Big|_{x=0}. \tag{2.7b}$$

In the following, $h_M = 10$ m is used, but the value of b_n is extremely insensitive to reasonable choices of this parameter. The details of the above derivation follow those in Clarke (1977) or Brink (1982b), and are not presented here. The only new twist is that F_n and b_n are imaginary for $fc_n < 0$, i.e., trench waves.

For the following, the eigenvalue problem (2.5) is solved by resonance iteration with a 17 × 25 finite difference grid. Details of the procedure are given in Brink (1982a). Only the gravest mode ($n = 0$, in the MLE notation) long trench waves will be considered, partly because of difficulties in accurately resolving higher modes. Also, since the higher modes generally have very low phase speeds (MLE, MW) it appears likely that they will in practice be strongly modified by nonlinear effects.

The present approach to wind driving is dynamically equivalent to that used by MW. This can be seen most clearly by reformulating their barotropic problem in terms of pressure instead of streamfunction. In this case, the wind forcing enters through the coastal boundary condition instead of the field equation. In either case, excitation of trench waves (as opposed to surface Ekman transport) by x-independent winds requires the presence of an impermeable coastal boundary to disrupt the surface Ekman transport. This point should be borne in mind when considering the Aleutian trench example below, since the Aleutian island chain is not a solid barrier (e.g., Schumacher, *et al.*, 1982). Thus, the coupling coefficients b_n for wind driving of Aleutian trench waves will be gross overestimates, both here and in MW.

3. An interpretation

The primary effects of stratification on free trench waves can be deduced from examination of Rhines' (1970) simple bottom-intensified topographic wave solutions. Exact application of his theory to a realistic trench is not possible because of strongly nonuniform bottom relief and stratification, but qualitative application seems quite reasonable. Rhines' dispersion relation for an unbounded ocean is

$$\omega = \frac{N_0 \alpha l}{\kappa \tanh\mu},$$

where N_0 is the uniform Brunt–Väisälä frequency, α the (small) constant bottom slope, l the along-isobath wavenumber, and κ the scalar wavenumber

$$\kappa = (k^2 + l^2)^{1/2},$$

where k is the wavenumber in the cross-isobath direction. The effect of stratification is determined by the parameter

$$\mu = N_0 \bar{h} \kappa f^{-1},$$

where $\bar{h}$ is the average depth. When $\mu \ll 1$, the solution essentially becomes a barotropic topographic Rossby wave governed by

$$\omega \approx \frac{f \alpha l}{\bar{h}\kappa^2},$$

and the motions are nearly depth-independent. On the other hand, when $\mu \gtrsim 2$, the motions become strongly bottom-trapped and

$$\omega \approx \frac{N_0 \alpha l}{\kappa}.$$

Since μ is proportional to the wavenumber κ, sufficiently long waves can approach the barotropic limit, but sufficiently short waves are always baroclinic for any reasonable choice of N_0, h and f. These qualitative properties can all be expected to carry over to realistic trench waves.

As a gross measure of the effects of stratification, the parameter $S^{1/2}$ can be constructed by analogy with μ or with Huthnance's (1978) scaling. First, notice that since trench waves are standing modes in the cross-isobath direction, k^{-1} must be of the order of L (the distance from the trench axis to the outlying flat-bottom ocean) for gravest mode trench waves. Further if attention is confined to long trench waves,

$$lL \ll 1,$$

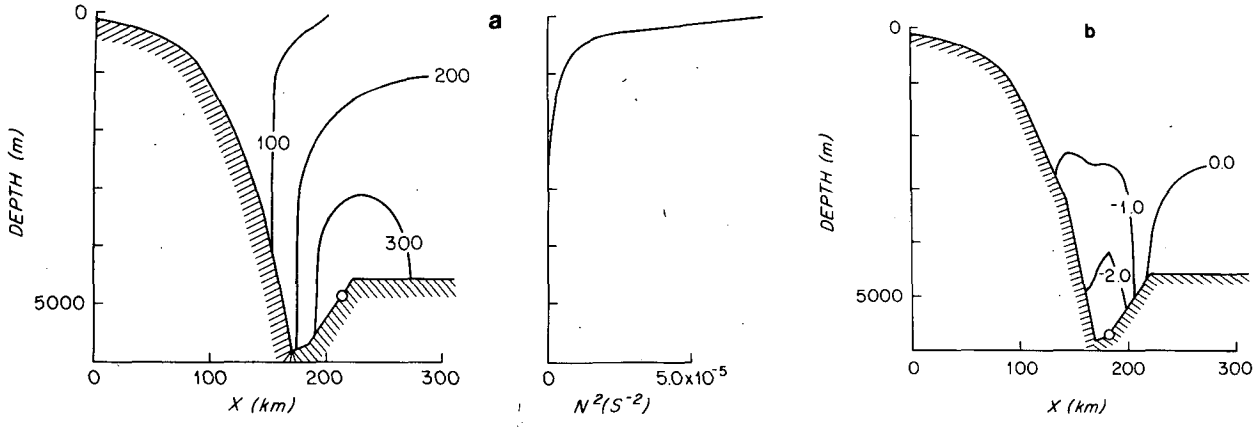

FIG. 1. Long-wave modal structure for the gravest mode trench wave off Peru. Units are arbitrary, but are set so that if p is in dyn cm^{-2}, v is in cm s^{-1}. Small circles denote extrema in the fields. (a) Pressure p. Also shown is the N^2 profile, averaged at 300 m increments. Note that $N^2 > 0$ for all depths. (b) Alongshore velocity v.

then

$$\kappa \sim L^{-1}$$

and

$$S^{1/2} = \frac{\bar{N} h_\infty}{fL}, \tag{3.1}$$

where $\bar{N}$ is the depth averaged buoyancy frequency and h_∞ the water depth far offshore. This parameter can be thought of as approximately the ratio of the first deep-sea internal Rossby radius of deformation to the trench width. By analogy with Rhines' (1970) results, large $S^{1/2}$ implies strong baroclinicity and $S^{1/2} \to 0$ (for finite $\bar{N}$) represents the barotropic limit.

The remainder of this paper will consider the effects of stratification for two cases representing widely differing degrees of baroclinicity. The examples are the Peru trench (MLE, $S^{1/2} = 6.3$) and the Aleutian trench (MW, $S^{1/2} = 1.4$). In both cases, modifications to wave behavior and some implications will be discussed.

4. Two examples

a. *The Peru trench*

The long wave $n = 0$ modal structure displayed in Fig. 1 was calculated using the topography given by MLE, stratification data provided by A. Huyer, and a value $f = -2.52 \times 10^{-5}$ rad s^{-1} (10° S). The present topography varies slightly from that in MLE, because of the inability of the finite difference grid to duplicate MLE's exponential functions exactly. The stratification parameter, $S^{1/2} \approx 6.3$, suggests that baroclinic effects should be extremely important, as indeed they are. The long wave phase speed c_0 is 51 cm s^{-1}, as compared to the barotropic value of 31 cm s^{-1}. Aside from the change in phase speed, the modal structure is also affected. Specifically, the wave is strongly bottom trapped: surface alongshore velocity directly above the trench axis ($x \approx 180$ km) is only about 7% of its value at the bottom.

One result of the strong bottom trapping is that the wave signal in coastal sea level is severely reduced from the barotropic case. Specifically, a 1 cm elevation of coastal sea level will correspond to a −450 cm s^{-1} particle velocity at the trench bottom where the alongshore velocity is a maximum. For convenience, we define

$$\gamma|\zeta| = \max[|v_0|],$$

where ζ is the coastal sea level in cm, and $\max[|v_0|]$ is the maximum alongshore speed associated with the $n = 0$ mode. Thus, for the baroclinic Peru example, $\gamma = 450$ s^{-1} while for comparison, $\gamma = 2$ s^{-1} for the barotropic case. Based on MLE, and spectra provided by R. L. Smith (personal communication, 1982), the total variance in coastal sea level which MLE associated with trench waves is ~2.5 cm^2, which according to this model, translates into maximal bottom particle speeds of ~710 cm s^{-1}. This value, about 14 times the wave phase speed, is clearly too large to be reasonable. It appears, then, that the coherence peak observed by MLE in coastal sea level must be primarily due to some other phenomenon.

This disqualification is unfortunate, because other aspects of the present model do compare well with the MLE observations. For example, MLE reported a phase velocity of 63 cm s^{-1}, which agrees far better with the baroclinic result than the barotropic. Also, their observed high coherence occurs at frequencies as high as 0.045 cpd. This is higher than the barotropic cutoff (zero group velocity) frequency, but still within the nearly nondispersive range of the baroclinic trench wave.

Finally, consider the non-resonant efficiency of wind driving of the long gravest mode trench wave. A direct comparison with the resonant results of MW is avoided because of the sensitivity to free-wave speed and to bottom friction. Further, only a quasi-steady example is used since an initial value problem

TABLE 1. Parameter comparison for various $n = 0$ long trench-wave calculations.

Case	c_0 (cm s^{-1})	$S^{1/2}$	r (cm^{-1})	γ (s^{-1})
Peru barotropic	31	—	13×10^{-7}	2
Peru baroclinic	51	6.3	0.79×10^{-7}	450
Aleutian barotropic	−258	—	1.9×10^{-7}	14
Aleutian baroclinic	−264	1.4	2.3×10^{-7}	15

would only add transients having a comparable amplitude. The wind stress is given as

$$\tau_0^y = Te^{i\omega t}, \tag{4.1}$$

where $\omega \ll f$, in accord with the long wave approximation. Then, the maximum alongshore speed associated with the $n = 0$ mode is the largest mode 0 contribution to $(\rho_0 f)^{-1} p_x$:

$$|v_M| = (\rho_0 f)^{-1} \phi_0 \max[|F_{0x}|], \tag{4.2a}$$

where from (2.7a) and (4.1)

$$\phi_0 = i(c_0 b_0 T/\omega) e^{i\omega t}, \tag{4.2b}$$

so that

$$|v_M| = \left| \frac{T}{\rho_0} \frac{r}{\omega} e^{i\omega t} \right|, \tag{4.2c}$$

where the definition of r follows from (4.2a) and (4.2b). Thus r is a measure of how efficiently the maximum particle velocity (as opposed to the overall mode) is excited, and is intended to be a measure of the best possible observability of nonresonant driving. In the crude overall sense of modal total kinetic ($\iint \frac{1}{2}\rho_0 v^2 dz dx$) plus potential ($\iint \frac{1}{2} g^2 N^{-2} \rho_0^{-1} \rho^2 dz dx$) wave energy per unit length of coast, the $n = 0$ trench wave with stratification is less efficiently excited than the barotropic $n = 0$ wave by factors of 490 and 1.3 for the Peru and Aleutian (see below) examples, given driving of the form (4.1). (The energy ratios are readily calculated knowing b_0, f, N^2 and the free wave modal structure for each example.) This is in accord with the intuitive idea that bottom trapped modes should not be efficiently excited by a surface wind stress. Values of c_0, $S^{1/2}$, r and γ are presented in Table 1. Using the tabulated value of r, a 1 dyne cm^{-2} wind fluctuation at a 20-day period will produce a maximum current of 0.02 cm s^{-1} associated with the $n = 0$ Peru mode. The 20-day period was taken as long enough to allow trench waves to exist, but short enough to allow the neglect of planetary beta. Finally, it should be noted that resonant response could be a good deal stronger, depending however upon dissipation.

b. *The Aleutian trench*

The modal structure shown in Fig. 2 was computed using MLE's topography, stratification data provided by W. B. Owens and $f = 11.4 \times 10^{-5}$ rad s^{-1} (51.5°N). In this case, $S^{1/2} \approx 1.4$, and baroclinicity is expected to be far less important than for the Peru trench. This is indeed the case: the baroclinic long wave phase speed is −264 cm s^{-1}, only slightly faster than the barotropic value of −258 cm s^{-1}. Also, although there is some bottom intensification, it is not as severe as in the Peru case: the surface alongshore velocity above the trench axis is ~48% of the bottom (maximal) value.

For numerical convenience, the trench topography for this example was truncated on the coastal side

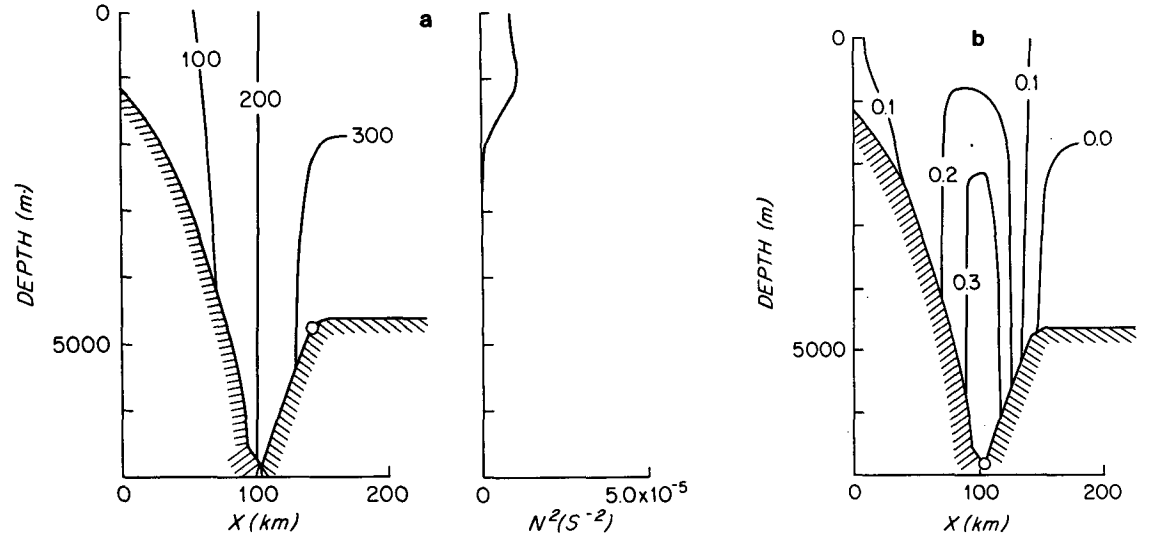

FIG. 2. Long-wave modal structure for the gravest mode trench wave off the Aleutians. Units are arbitrary, but are set so that if p is in dyn cm^{-2}, v is in cm s^{-1}. Small circles denote extrema in the fields. (a) Pressure p. Also shown is the N^2 profile, averaged at 300 m increments. Note that $N^2 > 0$ for all depths. (b) Alongshore velocity v.

relative to MW (that is, the coast is placed at $x = -100$ km in the MW notation instead if at $x = -150$ km as they used), so that estimates of r and γ will be too large by approximately a factor of two, relative to theirs. (The factor of 2 estimate arises from comparing barotropic mode results with the present topography with those using the MW topography. This is strictly geometric and is unrelated to the absence of a coastal barrier.) Relative to Peru, γ is larger (trench waves are less unlikely to be detectable in coastal sea level) and r is larger, meaning wind driving of *maximal* v, is more efficient. Nonetheless, a nonresonant 1 dyne cm^{-2} wind stress at a 20-day period still only drives $n = 0$ currents of 0.06 cm s^{-1}. Recall, however, that the Aleutian values of r are gross overestimates, because of the absence of an impermeable coast (Section 2).

5. Conclusions

Two examples of long, gravest mode trench waves in a stratified ocean have been presented. The modal structures show some structural similarities, despite the widely differing relative importance of baroclinicity. For example, extrema in v appear at or near the trench bottom in both cases, and maxima in p occur at the bottom near the offshore edge of the trench. Qualitatively consistent with Rhines' (1970) result, both examples show phase speed enhancement relative to the barotropic case and pronounced bottom trapping, although the degree varies markedly.

The present calculations take nothing away from trench waves as a viable physical phenomenon. However, it is fairly clear that baroclinic effects will generally not be negligible. Also, it appears that trench waves are unlikely to be observed in coastal sea level records, and that they will be inefficiently driven by nonresonant alongshore wind fluctuations.

Acknowledgments. Dr. A. Huyer and Dr. W. B. Owens kindly made their CTD data available to me for the calculations, and Dr. R. L. Smith provided me with sea level spectra from the Peru coast. Dr. D. C. Chapman provided several useful comments on the manuscript. This research was supported by the National Science Foundation through grant OCE-80-24116.

REFERENCES

Brink, K. H., 1982a: A comparison of long coastal trapped wave theory with observations off Peru. *J. Phys. Oceanogr.*, **12**, 897–913.

——, 1982b: The effect of bottom friction on low-frequency coastal trapped waves. *J. Phys. Oceanogr.*, **12**, 127–133.

Chapman, D. C., and M. C. Hendershott, 1982: Shelf wave dispersion in a geophysical ocean. *Dyn. Atmos. Oceans*, **7**, 17–31.

Clarke, A. J., 1977. Observational and numerical evidence for wind-forced coastal trapped waves. *J. Phys. Oceanogr.*, **7**, 231–247.

Gill, A. E., and E. H. Schumann, 1974: The generation of long shelf waves by the wind. *J. Phys. Oceanogr.*, **4**, 83–90.

Huthnance, J. M., 1978: On coastal trapped waves: Analysis and numerical calculation by inverse iteration. *J. Phys. Oceanogr.*, **8**, 74–92.

Mysak, L. A., and A. J. Willmott, 1981. Forced trench waves. *J. Phys. Oceanogr.*, **11**, 1481–1502.

——, P. H. LeBlond and W. J. Emery, 1979: Trench waves. *J. Phys. Oceanogr.*, **9**, 1001–1013.

Rhines, P. B., 1970. Edge-, bottom-, and Rossby waves in a rotating stratified fluid. *Geophys. Fluid Dyn.*; **1**, 273–302.

Schumacher, J. D., C. A. Pearson and J. E. Overland, 1982: On exchange of water between the Gulf of Alaska and the Bering Sea through Unimak Pass. *J. Geophys. Res.*, **87**, 5785–5795.